Roles of Conformational and Positional Adaptability in Structure-Based Design of TMC125-R165335 (Etravirine) and Related Non-nucleoside Reverse Transcriptase Inhibitors That Are Highly Potent and Effective against Wild-Type and Drug-Resistant HIV-1 Variants

Kalyan Das,[†] Arthur D. Clark, Jr.,[†] Paul J. Lewi,[‡] Jan Heeres,[‡] Marc R. de Jonge,[‡] Lucien M. H. Koymans,[‡] H. Maarten Vinkers,[‡] Frederik Daeyaert,[‡] Donald W. Ludovici,[§] Michael J. Kukla,[§] Bart De Corte,[§] Robert W. Kavash,[§] Chih Y. Ho,[§] Hong Ye,[§] Mark. A. Lichtenstein,[§] Koen Andries,[⊥] Rudi Pauwels,[⊥] Marie-Pierre de Béthune,[⊥] Paul L. Boyer,[#] Patrick Clark,[#] Stephen H. Hughes,[#] Paul A. J. Janssen,[‡,||] and Eddy Arnold*[,†]

Center for Advanced Biotechnology and Medicine and Department of Chemistry and Chemical Biology, Rutgers University, Piscataway, New Jersey 08854, Center for Molecular Design, Janssen Pharmaceutica NV, Vosselaar, Belgium, Janssen Research Foundation, Spring House, Pennsylvania, Tibotec, 2800 Mechelen, Belgium, and HIV Drug Resistance Program, NIH National Cancer Institute—Frederick, Frederick, Maryland 21702

Received November 4, 2003

Anti-AIDS drug candidate and non-nucleoside reverse transcriptase inhibitor (NNRTI) TMC125-R165335 (etravirine) caused an initial drop in viral load similar to that observed with a five-drug combination in naïve patients and retains potency in patients infected with NNRTI-resistant HIV-1 variants. TMC125-R165335 and related anti-AIDS drug candidates can bind the enzyme RT in multiple conformations and thereby escape the effects of drug-resistance mutations. Structural studies showed that this inhibitor and other diarylpyrimidine (DAPY) analogues can adapt to changes in the NNRTI-binding pocket in several ways: (1) DAPY analogues can bind in at least two conformationally distinct modes; (2) within a given binding mode, torsional flexibility ("wiggling") of DAPY analogues permits access to numerous conformational variants; and (3) the compact design of the DAPY analogues permits significant repositioning and reorientation (translation and rotation) within the pocket ("jiggling"). Such adaptations appear to be critical for potency against wild-type and a wide range of drug-resistant mutant HIV-1 RTs. Exploitation of favorable components of inhibitor conformational flexibility (such as torsional flexibility about strategically located chemical bonds) can be a powerful drug design concept, especially for designing drugs that will be effective against rapidly mutating targets.

Introduction

Emergence of drug-resistant viral variants in HIV-1-infected patients is a primary cause of treatment failure. Treatment with combinations of potent antiviral agents[1] targeting the viral enzymes reverse transcriptase (RT) and protease, termed highly active antiretroviral therapy (HAART), has been more successful than monotherapeutic regimens. There are, however, problems with drug toxicity and multidrug resistance after prolonged therapy. Non-nucleoside RT inhibitors (NNRTIs), as components of HAART, have the advantage that they are minimally toxic; however, there are significant problems with the development of NNRTI resistance.

Selective screening of the compound library in cell culture at Janssen Pharmaceutica in 1987, followed by a directed lead optimization program, led to the discovery of the first NNRTIs, the TIBO compounds.[2] The first-generation NNRTIs tivirapine, a TIBO derivative,[3] and loviride, an α-APA derivative,[4] were effective against wild-type HIV-1 but had significantly lower potency when tested against common NNRTI-resistant mutants. As chemical modifications were introduced in these TIBO and α-APA derivatives, a systematic structure-based molecular modeling study played a key role in understanding the three-dimensional structure−activity relationships (3DSAR) in these two chemically distinct series. This information was used for predicting NNRTI potency against both wild-type and NNRTI-resistant HIV-1 variants and in designing new NNRTIs effective against a wide range of HIV-1 variants.

Crystal structure analysis of HIV-1 RT has revealed important features of the enzyme's structure and function, including details of NNRTI binding. The structures

* Correspondence and requests for materials should be addressed to Eddy Arnold, CABM & Rutgers University, 679 Hoes Ln., Piscataway, NJ 08854 [e-mail arnold@cabm.rutgers.edu; phone (732) 235-5323; fax (732) 235-5788].

[†] Rutgers University.

[‡] Janssen Pharmaceutica NV.

[§] Janssen Research Foundation.

[⊥] Tibotec.

[#] NIH National Cancer Institute—Frederick.

[||] We dedicate this paper to the memory of Dr. Paul Adriaan Jan Janssen (1926−2003). Dr. Paul, as he was known to friends and colleagues, worked tirelessly to lead an assault on the worldwide AIDS epidemic, starting in 1987 with the discovery of the TIBO compounds, the first reported NNRTIs, and culminating with the discovery and development of the DAPY analogues, which show great promise for effective treatment and prevention of HIV infection. With his unique insights and approach to research, Dr. Paul guided the discovery and development of more than 75 drugs in areas including psychiatry, anesthesiology, mycology, parasitology, allergy, and gastroenterology. Friends of the humble Dr. Paul will remain inspired by his warmth, creativity, and compassion for all.

10.1021/jm030558s CCC: $27.50
Published on Web 04/06/2004

include unliganded HIV-1 RT,[5−7] RT in complexes with nucleic acid substrates [dsDNA,[8,9] dsDNA/dNTP,[10] and RNA/DNA[11]] and with different NNRTIs [such as nevirapine,[12,13] delavirdine,[14] efavirenz,[15,16] HBY 097,[17] and phenylethylthiazolylthiourea (PETT)[18,19]]. As a part of this project, we determined the X-ray crystal structures of tivirapine and loviride in complexes with wild-type HIV-1 RT and tivirapine with the Tyr181Cys mutant.[20−22] These structures provided information on the effects of substrate and inhibitor binding on the enzyme, snapshots of its functional conformations, information on the roles of resistance mutations, etc.

Key design features learned from structural studies include the following:

(1) Despite major chemical differences among the first-generation NNRTIs tivirapine, loviride, and nevirapine, all three bind to HIV-1 RT in a hydrophobic pocket (the non-nucleoside inhibitor-binding pocket, or NNIBP) with a common binding mode.[12,21] We termed this mode of binding "butterfly-like" [21] and defined Wing I, Wing II, and body/linker as modular segments to which different chemical substitutions or modifications could be made to yield new classes of NNRTIs. Wing I and Wing II generally contain aromatic rings that have $\pi-\pi$ interactions with aromatic amino acids (Tyr181, Tyr188, Phe227, Trp229, and Tyr318).

(2) The hydrophobic binding site or NNIBP is not present in structures of HIV-1 RT that do not have a bound NNRTI; this "closed form" of the NNIBP corresponds to a hydrophobic core that is collapsed in RT structures not containing an NNRTI but can be expanded to permit NNRTI binding to RT. The NNRTI-bound "open form" of the pocket might correspond to other states of RT required for viral replication. Expansion or opening of the NNIBP region involves large displacements of the aromatic side chains of Tyr181, Tyr188, and Trp229 and a rotation of the $\beta12-\beta13-\beta14$ sheet that results in a displacement of the "primer grip" in the direction the template-primer translocates following nucleotide incorporation.[22,23]

(3) The NNIBP is elastic, and its conformation depends on the size, specific chemical structure, and binding mode of the NNRTI; the overall structure of RT has segmental flexibility that also varies according to the nature of the bound NNRTI. Limits to the pocket's flexibility are not fully understood; this makes accurate predictions of the structures of HIV-1 RT/NNRTI complexes very challenging with the available molecular modeling techniques. Reliable molecular modeling of HIV-1 RT/NNRTI complexes requires experimentally determined structures of related RT/NNRTI complexes.

(4) The NNRTI-resistance mutations Tyr181Cys and Tyr188Leu directly affect NNRTI binding by altering protein−inhibitor interactions and reducing favorable $\pi-\pi$ interactions. The Leu100Ile mutation probably causes steric interference between the β-branched isoleucine and a bound NNRTI. The Gly190Ala mutation might cause resistance through steric conflict of the methyl side chain and the bound NNRTIs. The NNRTI-resistance mutation Lys103Asn indirectly affects NNRTI potency by stabilizing the closed form of the NNIBP through the formation of a hydrogen bond between the Asn103 side-chain amide and the Tyr188 phenoxyl oxygen, reducing the rate of inhibitor entry.[24] NNRTIs with some degree of conformational freedom, that can adapt to mutation-induced changes in the pocket, retain potency against some of the key drug-resistant HIV-1 variants.[17,22]

(5) Inhibitor binding can be stabilized, even in the presence of drug-resistance mutations, by optimizing interactions with amino acid residues in the NNIBP that are highly conserved, such as Trp229 (part of the "primer grip", required for positioning of nucleic acid during polymerization[8]).

(6) Molecular modeling analysis of the RT/NNRTI structures suggested that potent inhibitors tend to be bound in the NNIBP in low-energy conformations.

Molecular modeling and chemical synthesis driven by these ideas resulted in the discovery of diarylpyrimidine (DAPY) analogues that have shown promise in Phase I/II clinical trials. Overall, the in vitro potency profiles of the two DAPY derivatives, TMC120-R147681 (dapivirine) and TMC125-R165335 (etravirine), are better than those of all currently approved NNRTI drugs[25,26] (Table 1). Phase I/II clinical trials with treatment-naïve patients receiving twice daily doses of either 50 mg or 100 mg of TMC120-R147681[27] or of 900 mg of TMC125-R165335[28] showed decreases in mean viral load (RNA copies/mL) of about 1.5 $\log_{10}$ and 1.9 $\log_{10}$ (comparable to the drop in viral load by a combination of five approved anti-AIDS drugs), respectively, after one week of treatment. TMC125-R165335 was also effective in reducing HIV-1 viral load in NNRTI-experienced patients harboring efavirenz-resistant virus.[29]

Here we describe the path leading to the discovery of the DAPY drug candidates TMC120-R147681 and TMC125-R165335 from a structural perspective. The analysis suggests that inhibitors with selected conformational degrees of freedom, such as torsional flexibility around strategically located chemical bonds, can compensate for the effects of drug-resistance mutations. Using inhibitor flexibility in designing drugs to overcome the effects of resistance mutations has broader implications for diseases where drug resistance is a primary concern.

Results and Discussion

Structures of ITU, DATA, and DAPY Compounds in Complex with HIV-1 RT. Crystal structures of HIV-1 RT in complexes with six different inhibitors are described here (Table 2), representing the imidoylthiourea (ITU), diaryltriazine (DATA), and DAPY classes of NNRTIs, including the potent clinical candidates TMC120-R147681 and TMC125-R165335. The inhibitors were systematically tested[30,31] against a large number of HIV-1 clinical isolates, and potency correlations with structural and molecular modeling data guided the design and development process.[32]

Systematic variations of α-APA derivatives, first-generation NNRTIs, yielded the ITU compounds[33] (R100943 in Scheme 1). In terms of the butterfly model,[21] the ITU compounds were obtained by extending the linker (or body) connecting the two aryl side groups of the α-APA framework. Optimizing the chemical compositions of the side groups on the basis of structure−activity relationships (SAR) yielded compounds with 2,6-dichlorophenyl (Wing I) and 4-cyanoanilino (Wing II) rings. ITU compounds, which are more flexible than

Table 1. Potency (EC_{50} Values in μM) of Janssen NNRTIs Loviride, R100943, R120393, R129385, TMC120-R147681 (dapivirine), TMC125-R165335 (etravirine), and R185545 against Wild-Type and NNRTI-Resistant HIV-1 Strains Compared to that of Currently Approved NNRTI Drugs Nevirapine, Delavirdine, and Efavirenz[a]

	IIIB	Leu100Ile	Lys103Asn	Val106Ala	Tyr181Cys	Tyr188Leu	Gly190Ala
Loviride	0.005	0.05	1.26	1	15.8	50.1	2.51
Delavirdine	0.016	3.467	1.697	2.245	1.336	0.178	0.038
Nevirapine	0.085	0.638	2.467	2.41	5.351	>100.0	3.465
R100943	0.003	0.513	0.589	0.382	0.511	0.318	0.002
R106168	0.002	0.293	0.041	0.026	0.277	0.431	0.001
R120393	0.003	1	0.063	0.063	0.25	1	0.003
R129385	0.003	0.32	0.079	0.1	0.25	3.2	–
TMC120-R147681	0.001	0.016	0.004	0.003	0.008	0.04	0.001
TMC125-R165335	0.002	0.003	0.001	0.002	0.006	0.003	0.001
R185545	0.004	0.002	0.004	0.002	0.006	0.006	0.001
Efavirenz	0.001	0.038	0.039	0.36	0.002	0.138	0.011

[a] Color codes: orange, EC_{50} > 0.1 μM; yellow, 0.1 > EC_{50} > 0.01 μM; and light yellow, EC_{50} < 0.01 μM.

Table 2. X-ray Diffraction Data and Refinement Statistics

	HIV-1 RT/ R100943	HIV-1 RT/ R120393	HIV-1 RT/ R129385	HIV-1 RT/ TMC120-R147681	Lys103Asn mutant RT/ TMC125-R165335	HIV-1 RT/ R185545
			X-ray Diffraction Data			
PDB code	1S6P	1S9G	1S9E	1S6Q	1SV5	1SUQ
X-ray source	CHESS F1	CHESS F1	CHESS F1	BNL X25	CHESS F1	APS BMD
wavelength (Å)	0.908	0.918	0.918	0.921	0.916	1.00
space group	*C*2	*C*2	*C*2	*C*2	*C*2	*C*2
cell constants (a,b,c in Å; β in °)	226.7, 69.4, 104.3 Å; 107.0°	223.6, 68.3, 103.0 Å; 107.5°	226.8, 69.3, 104.1 Å; 106.7°	228.3, 69.6, 105.3 Å; 106.3°	222.5, 67.7, 103.3 Å; 107.5°	226.1, 69.7, 104.23 Å; 106.8°
resolution range (Å)	40.0−2.9	40−2.8	40.0−2.6	40.0−3.0	40.0−2.85	40.0−3.0
no. of unique reflections (no. of observation)	31 923 (92 234)	33 445 (96 989)	46 005 (153 480)	30 428 (79 715)	32 405 (89 999)	29 837 (124 234)
completeness (in last shell)	91.9 (80.5)	90.3 (79.3)	95.9 (89.3)	94.8 (78.4)	94.8 (83.2)	95.0 (73.3)
R-merge (in last shell)	0.098 (0.37)	0.083 (0.29)	0.085 (0.37)	0.096 (0.32)	0.112 (0.35)	0.078 (0.41)
I/σ cutoff	0.0	0.0	0.0	0.0	−0.5	−1.0
			Refinement Statistics			
total no. of atoms (inhibitor/solvent molecules)	8169 (22/151)	8109 (27/141)	8234 (24/181)	8053 (24/0)	7950 (28/0)	8055 (29/0)
resolution range (Å)	20.0−2.9	20.0−2.8	20.0−2.6	20.0−3.0	20.0−2.9	20−3.0
no. of reflections (R_{free} set)	30 218 (1542)	32 863 (1666)	44 669 (2236)	29 295 (1482)	31 269 (1578)	28 520 (1404)
completeness (%)	89.8	89.0	93.3	91.6	95.4	91.1
cutoff criteria	$\|F\| < 1.0\sigma(\|F\|)$	$\|F\| < 1.0\sigma(\|F\|)$	$\|F\| < 1.0\sigma(\|F\|)$	$\|F\| < 1.0\sigma(\|F\|)$	$\|F\| < 1.0\sigma(\|F\|)$	$\|F\| < 1.0\sigma(\|F\|)$
R_{cryst}	0.245	0.241	0.253	0.246	0.255	0.262
R_{free}	0.312	0.312	0.316	0.294	0.326	0.325
RMS deviations:						
bond lengths (Å)	0.012	0.012	0.015	0.013	0.013	0.011
bond angles (°)	1.84	1.88	2.0	1.84	1.93	1.8

their progenitors, inhibit wild-type HIV-1 at nanomolar concentrations and potently inhibit several key NNRTI-resistant mutants (Table 1). The RT-bound conformation of the ITU derivative R100943 (Figure 1a) resembles a "U" or "horseshoe", in contrast to the "butterfly-like" shape of α-APA, TIBO, and nevirapine.[21] Comparison of the binding mode of R100943 with that of another class of thiourea NNRTIs, the PETT compounds,[18,19] reveals interesting differences (Figure 1b) despite their chemical similarities.

The serendipitous synthesis of a compound containing a triazine ring linking Wing I and Wing II, replacing the relatively unstable thiourea moiety of ITU derivatives, led to the development of the DATA series of NNRTIs.[34] The prototype DATA compound, R106168 (Scheme 1), was simple to synthesize and had an improved resistance spectrum (Table 1). Multiple substitutions and/or additions were made at various positions on all three rings and on the two linkers connecting the rings of the DATA derivatives.[34] Many of the

Scheme 1. Chemical Structures of Janssen NNRTIs: Tivirapine (TIBO), Loviride (α-APA), ITU (R100943), DATA (R106168, R120393, and R129385), and DAPY (TMC120-R147681 (dapivirine), TMC125-R165335 (etravirine), and R185545) Analogues

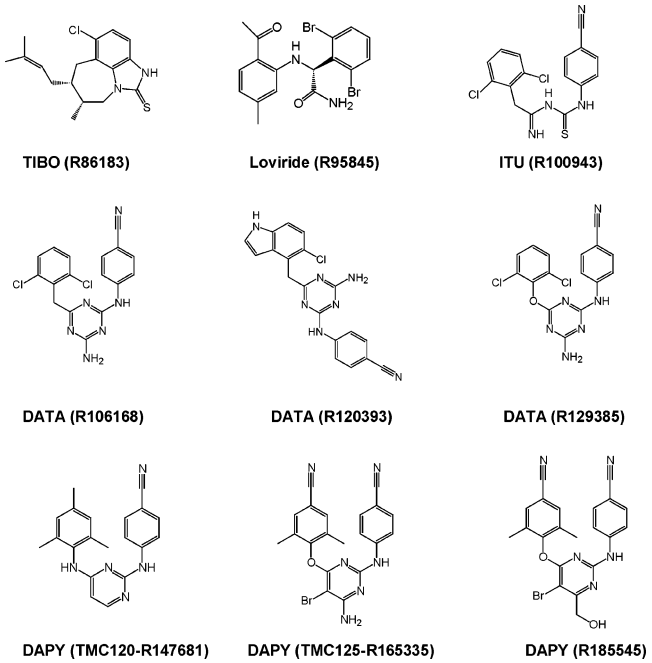

DATA derivatives have nanomolar EC_{50} against wild-type HIV-1 RT and bind to HIV-1 RT in a horseshoe conformation, as seen with the ITU compounds. The structure of the HIV-1 RT/R129385 complex, determined at 2.6 Å resolution, is used as the representative structure for HIV-1 RT/DATA complexes. The two outer rings (2,6-dichlorophenoxy and 4-cyanoanilino) of R129385 occupy positions in the binding pocket similar to the corresponding outer rings of the ITU derivatives. In the central portion of DATA compounds, the triazine ring, which replaced the thiourea group of ITU derivatives, is sandwiched between the side chains of Leu100 and Val179. The aromatic triazine ring substitution removed a number of potentially redundant torsional degrees of freedom in the body moiety while preserving the flexibility of the connections between the triazine ring and the wings. The restriction of the unwanted flexibility within a moiety is expected to be entropically favorable, which may explain why DATA analogues are, in general, more potent than their precursors against wild-type and NNRTI-resistant HIV-1 strains.

Substitutions in the Wing I moiety of DATA analogues can have major effects on potency. The DATA analogue R120393 was designed with Wing I as a chloroindole moiety (Scheme 1) to make additional interactions with the side chain of conserved Trp229. R120393 retains potency similar to that of its progenitor, R106168, against many mutants but is less potent against Leu100Ile and Tyr188Leu (Table 1). The crystal structure of the HIV-1 RT/R120393 complex, determined at 2.8 Å resolution, showed that this DATA analogue binds unexpectedly with a more extended conformation (Figure 2). Interaction of the chloroindole (Wing I) of R120393 with the NNIBP apparently dominates this binding mode, leading to the indole ring being positioned ∼2 Å deeper in the pocket than the Wing I of other DATA analogues. This repositioning of the chloroindole Wing I has the effect of forcing the central triazine ring ∼3 Å deeper into the pocket, compared to R129385 (Figures 2b and 3a), so binding of R120393 in the horseshoe mode would result in steric conflict between Wing II and pocket residues. The NNIBP is expanded in the region surrounding the bulkier Wing I in the R120393 complex structure relative to the R129385 complex. The inhibitor−protein interaction with the main-chain carbonyl oxygen of Lys101, an interaction that is conserved for bound DATA, ITU, TIBO, and some other classes of NNRTIs, is not present for R120393. The exocyclic amino group at the 4-position of the triazine ring of R120393 is located in the vicinity of the Lys101 carbonyl oxygen but is too far away (4.7 Å) to form a hydrogen bond. A bridging water molecule in the pocket interacts with the NH group (linking the triazine and cyanoanilino rings) of R120393 and the Tyr188 main-chain carbonyl oxygen. Crystal structures of HIV-1 RT/NNRTI (DATA) complexes, in particular of RT/R120393, suggest that the DATA compounds have the ability to bind in alternative modes in the NNIBP, due to their conformational flexibility. Access to multiple binding modes permits a wider range of inhibitor modifications that can retain activity and provides opportunities for evading drug-resistance mutations.

Substantial differences in the potency of the inhibitors against HIV-1 variants were observed upon (1) varying the size and chemical composition of Wing I, (2) permuting the triazine ring nitrogens and replacing the triazine nitrogen atoms with carbons, and (3) substituting the two linker groups (connecting the rings) with NH, O, and CH_2. Replacement of the central triazine ring with a pyrimidine was a synthetically straightforward modification that was also suggested by molecular modeling. The resulting DAPY compounds were found to be more potent than DATA compounds when tested against a broad spectrum of resistant mutants (Table 1). Molecular modeling suggested that replacing the exocyclic amino group at the 4-position of the triazine/pyrimidine ring with hydrogen would be favorable, leading directly to the synthesis of TMC120-R147681. Pyrimidine replacement of the triazine ring also enabled substitutions at the 5-position, including the bromine in TMC125-R165335.

Crystal structures of TMC120-R147681 and R185545 in complexes with HIV-1 RT revealed that these DAPY analogues, like most of the DATA compounds, adopt the horseshoe mode of binding (Figure 3b,d). There are important differences, however, in their conformations (Table 3) and specific positioning within the NNIBP. Differences in positioning of the various NNRTIs with respect to NNIBP residues were also observed among thiourea derivatives, the ITU and PETT analogues (Figure 1b), and the DATA derivatives.[35] Adaptation of NNRTIs to the binding pocket involves a combination of conformational adjustments ("wiggling") of and rotational and translational shifts ("jiggling") of the inhibitor within the binding pocket. Conformational variations of the DATA and DAPY derivatives result from changes in torsion angles $\tau 1$, $\tau 2$, $\tau 3$, and $\tau 4$ (Table 3); their compact structures also permit rotational and translational shifts within the binding pocket. Molecular modeling also suggested that, for most of the DAPY and DATA NNRTIs, the $\tau 1$ and $\tau 2$ angles can be varied

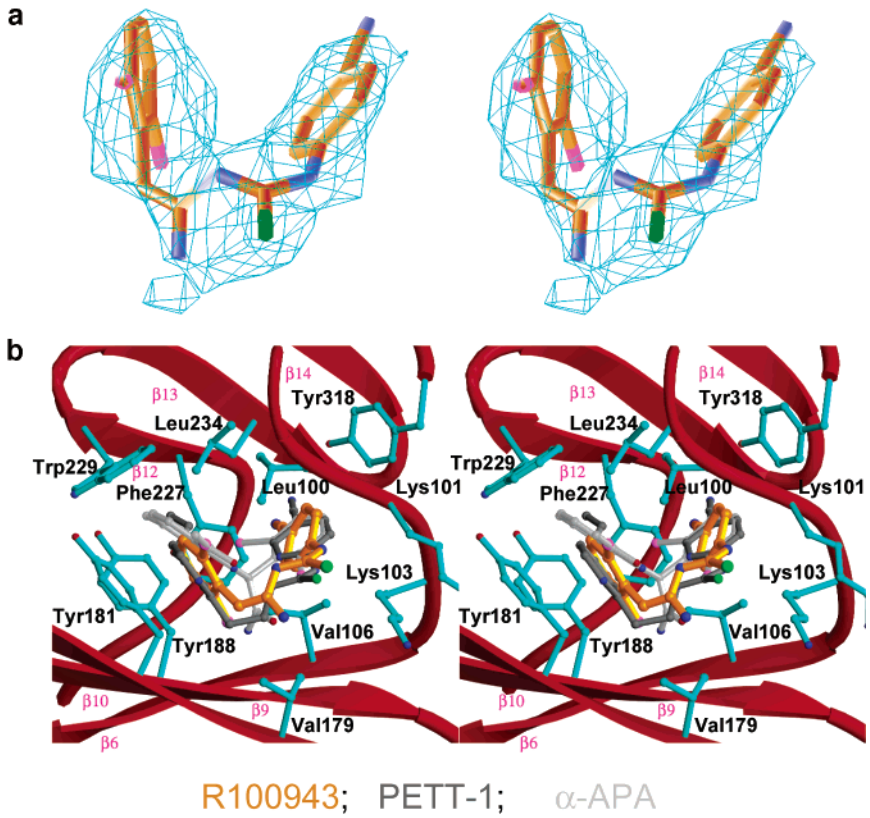

Figure 1. (a) Section of a 2.9 Å resolution simulated annealing omit map ($2mF_{obs} - DF_{calc}$; 1.0σ contours) for the HIV-1 RT/R100943 structure, covering the inhibitor R100943. (b) Binding mode of R100943 compared with those of loviride[20] and PETT-1.[19] The protein atoms shown are from the HIV-1 RT/R100943 complex, with the inhibitor shown in gold. Loviride (silver) and PETT-1 (gray) are superimposed on the HIV-1 RT/R100943 structure by aligning Cα atoms of the NNIBP region (p66 residues 105−110, 178−191, and 225−235 from secondary structural elements β6, β9, β10, β12, β13, and β14).

without encountering significant energy barriers (Figure 4). Apparently, as will be discussed later, DATA and DAPY analogues can change conformation (wiggle) and reorient and reposition (jiggle) in response to changes in the NNIBP caused by mutations, and this adaptability may help to explain their ability to inhibit HIV-1 RT carrying NNRTI-resistance mutations.

Structure of TMC125-R165335 in Complex with Lys103Asn Mutant HIV-1 RT. At a stage when obtaining crystals of HIV-1 RT/NNRTI complexes and X-ray diffraction data from the crystals had become relatively straightforward, even after trying hundreds of modifications of the crystallization conditions and variations in crystal treatment techniques, the wild-type HIV-1 RT/TMC125-R165335 crystals consistently diffracted X-rays only to about 6−8 Å resolution, even when high-intensity synchrotron radiation was used. It is possible that TMC125-R165335 binds RT in more than one binding mode and that the different corresponding RT conformations coexist in our crystals. This conformational heterogeneity could account for the low-resolution diffraction. Multiple modes of binding for the DAPY derivatives to HIV-1 RT were also detected[35] by principal component analysis of the relationship between NNRTI resistance profiles and the stereochemical and energetic features of the modeled HIV-1 RT/NNRTI complex structures. A recent molecular modeling study[36] on binding of TMC125-R165335 to HIV-1 RT predicted a difference of only 1.2 kcal/mol between the two lowest energy RT-bound conformations of the flexible enzyme.

We hypothesized that some of the NNRTI-resistant HIV-1 RT mutants might have fewer distinct binding modes for TMC125-R165335 than the wild-type enzyme would have, or could favor a particular binding mode, and that cocrystallization with mutants might yield better quality crystals. Pursuing this approach, we were delighted when dehydrated crystals of Lys103Asn RT/TMC125-R165335 complexes were obtained that diffracted X-rays to 2.9 Å resolution. The electron density corresponding to the inhibitor in the binding pocket, though well defined, was weaker than the electron density corresponding to the well-ordered amino acid residues of RT. The refined inhibitor has higher *B*-factors, particularly for the pyrimidine and 1,4-cyanophenyl rings, suggesting that the inhibitor may exhibit some degree of positional disorder. In the principal binding mode seen in the crystal (Figure 5), TMC125-R165335 is bound to Lys103Asn RT in a significantly different mode than R185545 and TMC120-R147681 (Figure 3) to wild-type HIV-1 RT. The central pyrimidine ring of TMC125-R165335 is sandwiched between the side chains of Leu100 and Asn103 and interacts with the main-chain atoms of amino acids 100−103 from p66. The side chain of Asn103 in Lys103Asn mutant RT has recently being predicted by a molecular modeling study[37] to contribute favorably to protein−ligand van der Waals interactions in binding of potent NNRTIs like efavirenz.

Molecular Simulations Support Multiple Binding Mode Hypothesis. We used molecular dynamics simulations, as implemented in the simulated anneal-

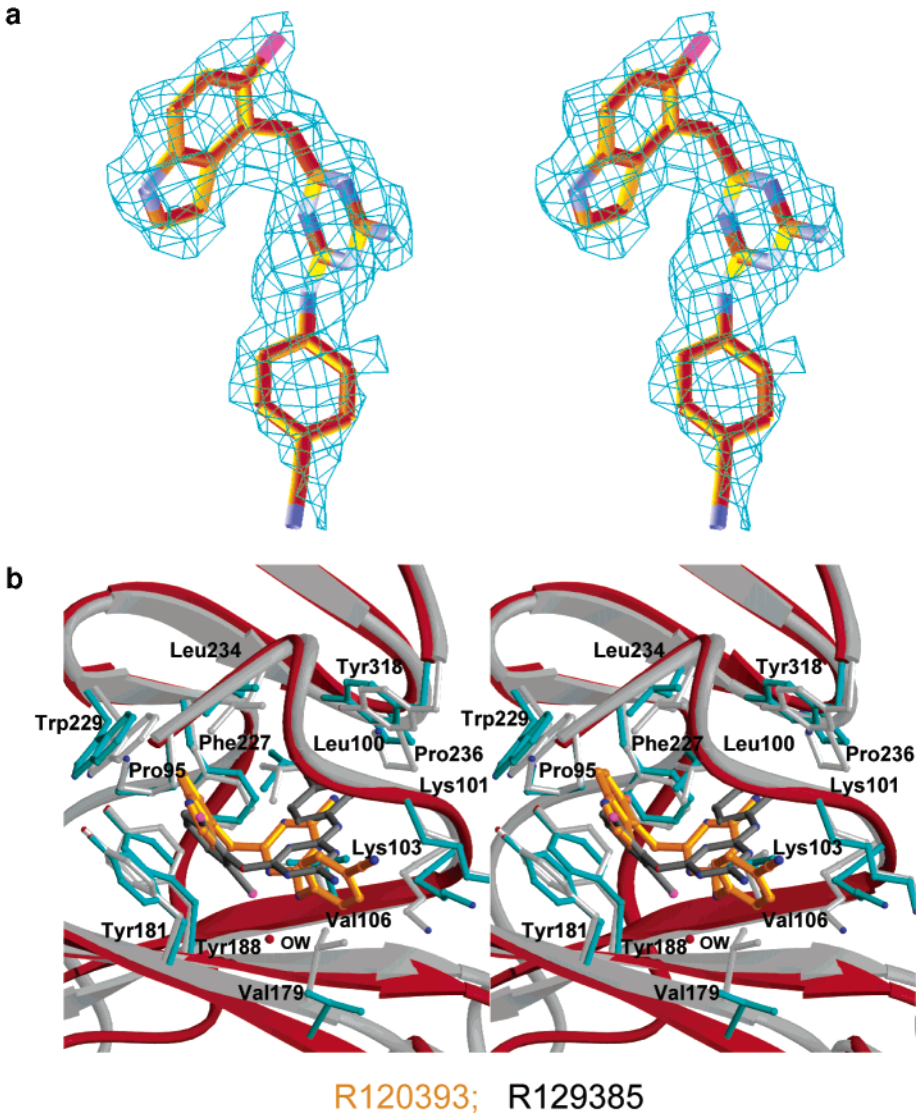

Figure 2. (a) "Seahorse" conformation of DATA analogue R120393 observed in its complex with HIV-1 RT, defined by electron density from a difference ($F_{obs} - F_{calc}$) map calculated on the basis of phase information from protein atoms prior to inclusion of the inhibitor in structure refinement. (b) Comparison of the mode of binding to HIV-1 RT of two DATA compounds R120393 (gold inhibitor with red ribbon and cyan side chains) and R129385 (gray inhibitor with silver ribbon and side chains) based on the alignment used in Figure 1b.

ing/slow cooling protocol in CNS 1.1,[38] to further examine the potential for DAPY NNRTIs to have multiple modes for binding to HIV-1 RT. Conformations of TMC125-R165335 obtained by this approach fell into discrete groups, including the conformation seen in the crystal structure of the Lys103Asn mutant HIV-1 RT/TMC125-R165335 (Figure 3c) complex and the extended conformation seen in the RT/R120393 complex structure (Figure 3a). Convergence of TMC125-R165335 to different conformations in the molecular dynamics calculations supports the hypothesis that the potency and resilience of DAPY NNRTIs is due to their ability to wiggle and jiggle within the pocket. Similar simulations were performed with the RT/R129385 and RT/TMC120-R147681 structures. The bound R129385 molecules converged closely to the position and conformation observed in the crystal structure. The TMC120-R147681 simulation yielded horseshoe conformations only, with greater torsion angle variation (wiggling) than for R129385 but considerably less than for TMC125-R165335. The trend for positional variations (jiggling) also follows the same order as for wiggling (TMC125-R165335 > TMC120-R147681 > R129385). The molecular dynamics results are also consistent with the relatively weaker electron density observed for TMC120-R147681 and TMC125-R165335, compared to R129385, which may be attributable to positional disorder of the bound inhibitors. The conformation for TMC125-R165335 predicted by a molecular modeling study[36] is closely related to but not superimposable on the inhibitor conformation in the Lys103Asn mutant RT/TMC125-R165335 complex structure. However, considering the flexibility of the inhibitor, the predicted conformation of TMC125-R165335[36] is achievable and could possibly be the predominant one when complexed with wild-type HIV-1 RT.

NNRTI Conformational Flexibility and Adaptation to Resistance Mutations. Resistance mutations associated with NNRTI treatment failure occur primarily in and around the NNIBP. Commonly observed NNRTI-resistance mutations include Leu100Ile, Lys103Asn, Tyr181Cys, Tyr188Leu, and Gly190Ala.[39,40]

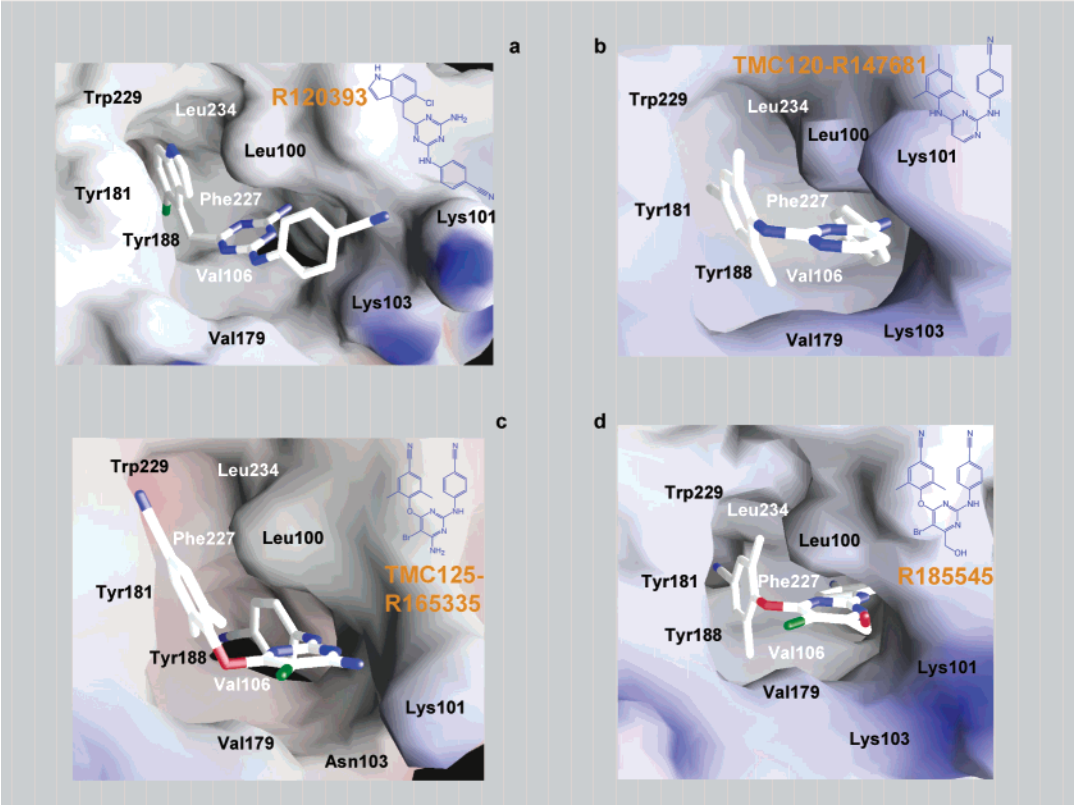

Figure 3. Binding modes of DATA and DAPY NNRTIs: (a) R120393, (b) TMC120-R147681, (c) TMC125-R165335, and (d) R185545 to HIV-1 RT (Lys103Asn mutant RT for TMC125-R165335). The electrostatic potential surfaces of the NNIBP were calculated using GRASP;[52] selected pocket residues were omitted to permit viewing into the pocket.

Table 3. Values of the Torsion Angles (τ1,τ2, τ3, and τ4) of Janssen NNRTIs Change To Accommodate Different Chemical Modifications or Substitutions

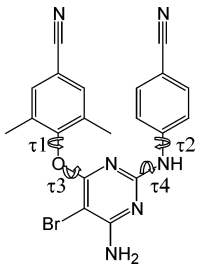

	torsion angles (°)			
	τ1	τ2	τ3	τ4
R100943	−65	−52	2	−2
R120393	−52	56	98	−144
R129385	−105	−15	−13	1
TMC120-R147681	−100	18	0	−14
R185545	−88	0	2	−15
TMC125-R165335	−102	85	−66	−14

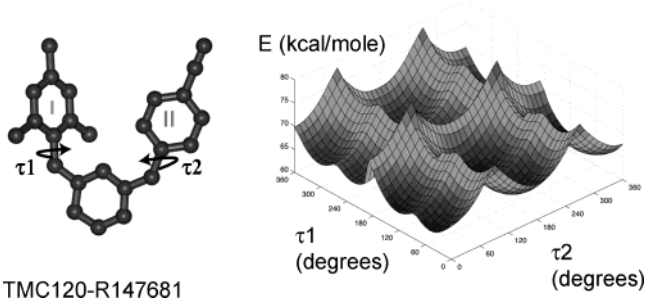

TMC120-R147681

Figure 4. Variation in conformational energy of TMC120-R147681 as a function of the torsion angles τ1 and τ2. The fairly shallow energetic barrier (especially for τ1 rotation) permits easy interconversion among inhibitor conformations. The DATA and DAPY compounds were predicted to have a similar energetic landscape.

Structural and molecular modeling studies of drug-resistant HIV-1 RT mutants, both in the presence and in the absence of bound NNRTIs,[15−17,22,24,37,41,42] have suggested possible mechanisms by which key mutations confer resistance to NNRTIs.

Gly190Ala mutation, which causes high-level resistance to loviride and HBY 097, has no significant effect on the potencies of the ITU, DATA, and DAPY inhibitors. This mutation was proposed to cause resistance[17] by filling a part of the binding pocket that would otherwise be occupied by the linker portion of the butterfly-shaped NNRTIs like loviride or by the quinoxaline ring of HBY 097. With the ITU, DATA, and DAPY inhibitors, a Cβ atom introduced by Gly190Ala mutation would point toward the central part of the inhibitors (a thiourea, triazine, or pyrimidine group). However, a minimum distance of 6.0 Å (5.4 Å for R120393) between the Cα atom of Gly190 and the central part of the current inhibitors suggests that there would be no serious steric conflict between an alanine at position 190 and the bound ITU, DATA, and DAPY analogues described here.

The amino acid residues Leu100,[37] Tyr181,[22] and Tyr188[17,41] form a portion of the hydrophobic core of the binding pocket that interacts with Wing I of the ITU, DATA, and DAPY NNRTIs. Mutation of one or more of these amino acids can affect inhibitor−protein interactions and the size, shape, and chemical environment of the binding pocket. Many of these changes are

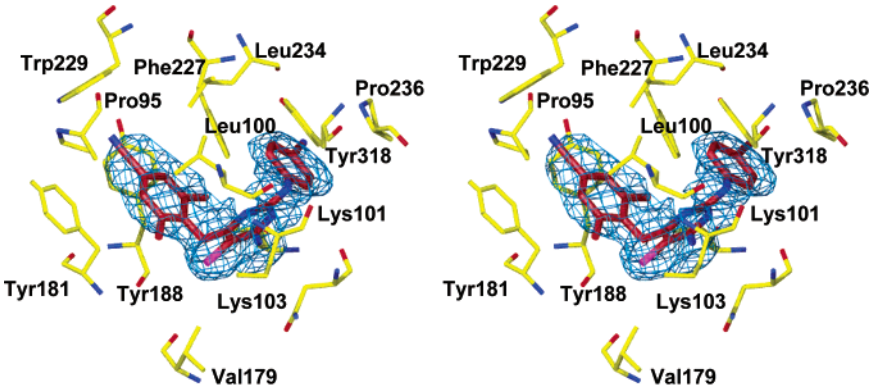

Figure 5. Difference Fourier electron density (1.8σ contours) defining the conformation of TMC125-R165335 when it is bound to Lys103Asn mutant HIV-1 RT.

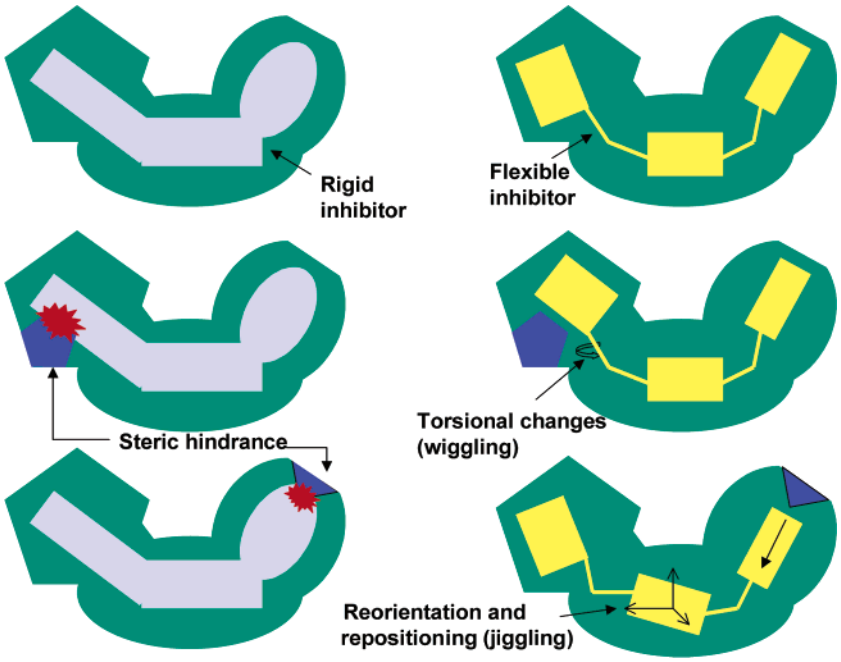

Figure 6. Schematic representation depicting how a flexible inhibitor is more effective than a rigid inhibitor in overcoming the effects of a resistance mutation.

expected to have direct effects on NNRTI binding. Previous structural studies have suggested that the Tyr181Cys[22,41] and Tyr188Leu[17] mutations affect the binding of an NNRTI by loss of favorable aromatic ring interactions. In contrast, the Lys103Asn mutation apparently affects the kinetics of the inhibitor-binding process by stabilizing the unbound state of RT via the generation of an additional hydrogen bond between the Tyr188 phenoxyl group and the Asn103 side chain.[24]

As has already been discussed, the DAPY NNRTIs have improved potency when compared to other NNRTIs, including nevirapine, delavirdine, and efavirenz (Table 1). Crystal structure and molecular modeling analyses have suggested a role for conformational flexibility in compensating for the effects of NNRTI-resistance mutations. Recent thermodynamic[43] and structural and molecular modeling studies[44] of HIV protease:inhibitor complexes found entopically and structurally favorable binding modes of a new generation of potent protease inhibitors to drug-resistant mutant enzymes. The thermodynamic study[43] also predicted that flexibility of a protease inhibitor is essential for its favorable binding to mutant enzymes. A classic lock and key model for inhibitor binding requires the ideal inhibitor to fill its complementary binding pocket, maximizing favorable interactions with the target. For targets (such as HIV enzymes) where escape mutations severely affect the potency of an inhibitor, resilience to resistance mutations requires that a drug adjust to the altered conformations of the pocket found in resistant mutants, in accordance with the "hand in a glove" paradigm (Figure 6).

Conformational changes in the DAPY/DATA NNRTIs (Figure 3) are achieved by variation of four torsion angles (τ1, τ2, τ3, and τ4), as indicated in Table 3. Torsion angles τ1 and τ2 can be easily varied with no significant energetic penalty (Figure 4). Changes in τ1 and τ2 cause conformational perturbations within the horseshoe mode, whereas changes in all four torsion angles are required for rearrangement from the horseshoe to the extended conformation seen with R120393 (Figure 3a, Table 3). Some of the DATA/DAPY inhibitors may bind using an extended conformation to accommodate changes in the binding pocket caused by some of the drug-resistance mutations.

Most of the ITU/DATA/DAPY NNRTIs bind to HIV-1 RT in the horseshoe mode. Changes in $\tau 1$ permit reorientation of Wing I in the hydrophobic NNIBP surrounded by the side chains of Pro95, Leu100, Tyr181, Tyr188, Trp229, and Leu234, or with mutated side chains at some of these positions in drug-resistant variants. There seems to be a favorable coupling of the torsion angles $\tau 1$ and $\tau 2$ in the DATA/DAPY analogues so that Wings I and II can orient themselves relative to each other (Figures 3 and 6). In other words, Wings I and II in a horseshoe conformation can be thought of as forming part of the binding site for each other. Changes in $\tau 2$, complementary to changes in $\tau 1$ (Table 3), position Wing II to have favorable interactions with Wing I and with the NNIBP residues. When Wing I reorients to accommodate to changes in the NNIBP caused by mutations, $\tau 1$ changes and there are compensatory changes in $\tau 2$ with only a modest energetic penalty (Figure 4). In the structure of the Lys103Asn mutant RT/TMC125-R165335 complex, the τ angles deviate from the usual values seen in a horseshoe conformation (Table 3). The twisted conformation of TMC125-R165335 (Figure 3c) in this mutant complex permits enhanced interactions (1) of the pyrimidine ring with side chains of Leu100 and Asn103, and (2) of Wing II with Tyr318 when compared with DATA/DAPY NNRTIs in horseshoe conformations.

Conclusions

The flexibility of highly potent DAPY analogues and easy interconversions among their related conformations (Figure 3) may help to explain their improved resilience to resistance mutations (Table 1) when compared with other NNRTI drugs and drug candidates. The chemical diversity of NNRTIs and the flexibility of the inhibitor-binding pocket provide opportunities as well as challenges for designing potent NNRTIs. The concept of exploiting conformational degrees of freedom to offset the effects of resistance mutations (Figure 6) may have broader implications for designing drugs against other rapidly evolving targets such as HIV protease[43] or for developing drugs against a common target from related organisms, like designing macrolide antibiotics to target a broader spectrum of bacterial ribosomes.[45]

Experimental Section

Abbreviations. 3DSAR, three-dimensional structure−activity relationships; DAPY, diarylpyrimidine; DATA, diaryltriazine; HAART, highly active antiretroviral therapy; ITU, imidoylthiourea; NNIBP, non-nucleoside inhibitor-binding pocket; NNRTI, non-nucleoside reverse transcriptase inhibitor; PETT, phenylethylthiazolylthiourea; RT, reverse transcriptase.

Anti-HIV Activity Measurement. Determination of the antiviral activity of compounds was done as described previously.[46] Briefly, various concentrations of the test compounds were brought into each well of a flat-bottom microtiter plate. Subsequently, HIV and MT4 cells were added to a final concentration of 200−250 50% cell culture infectious doses (CCID50)/well and 3×10^4 cells/well, respectively. After 5 days of incubation (37 °C, 5% CO_2), the cytopathic effect (CPE) of the replicating virus was determined by the tetrazolium colorimetric MTT method. The dose achieving 50% infection was defined as the EC_{50}.

Crystallization and Structure Determination. The inhibitors were crystallized using protocols described earlier.[47] The crystals grew to a size suitable for diffraction data collection within 4−7 days after microcrystal seeding. Typical rod-shaped crystals with dimensions $0.15 \times 0.2 \times 0.5$ mm were used for X-ray diffraction experiments. The crystals were dipped in mother liquor containing 20% glycerol (usually for 5−20 s depending on the NNRTI) and flash-cooled in a gaseous N_2 stream at 100 K. Crystals of HIV-1 RT/TMC125-R165335 consistently diffracted to ∼6−8 Å resolution. A crystal of Lys103Asn mutant HIV-1 RT/TMC125-R165335 complex in a hanging drop was dehydrated for two weeks over a well containing 40% PEG8000. The dehydrated crystal diffracted X-rays to 2.9 Å resolution. The diffraction data for the complexes were collected from one crystal of each type using synchrotron radiation sources at the Cornell High Energy Synchrotron Source (CHESS) F1 and Brookhaven National Laboratory (BNL) X25 beam lines. The data were processed and scaled using DENZO and SCALEPACK, respectively.[48] The previously reported HIV-1 RT/TIBO structure (PDB code 1HNV) was used as a template in obtaining molecular replacement solutions for the HIV-1 RT/R100943 complex structure. Rigid body refinement of the initial model, broken into 13 separate rigid segments (one fragment per subdomain except for two fragments each from p66 and p51 fingers and palm), reduced the starting *R*-factors by about 4−5%, indicating that interdomain and subdomain movements vary according to which NNRTI is bound. The final model for the complex was obtained after cycles of model building in O[49] and restrained refinements using XPLOR 3.843 and later using CNS 1.0.[38] Similar molecular replacement and refinement steps were used in obtaining the remaining five structures. The X-ray data, refinement statistics, and PDB accession numbers for all six HIV-1 RT/NNRTI complex structures are listed in Table 2.

Molecular Modeling. To search for other possible modes of binding, multiple low-energy conformations of NNRTIs were generated and docked into NNIBPs obtained from the crystal structures. The conformations of the NNRTIs were generated by means of a genetic algorithm that builds an initial population of conformers by exhaustively sampling rotatable bonds with a 60° step-size. Subsequently, point mutations were introduced as perturbations of rotamers, and various crossover offspring were generated and optimized. The low-energy forms (up to 7 kcal/mol higher in internal energy than the global minimum) were then docked into the NNIBP by means of a genetic algorithm that optimizes the nonbonded interactions (van der Waals, Coulomb, and hydrogen-bonding energy). The resulting set of RT-bound NNRTI conformations was then relaxed by geometry optimization, and the most favorable ones were retained (typically between one and four complex geometries are found within a few kilocalories per mole of internal energy). A force field based on MMFF94[50] and supplemented with a directional hydrogen-bonding term was used in searching, docking, and complex minimization calculations.

Furthermore, strategic chemical modifications of the NNRTIs, with improved biological activity, were modeled by means of a genetic algorithm.[51] This genetic algorithm uses the predicted potency of the compound as its fitness function. The potency prediction is based on correlation of computed interaction energies between inhibitors with known biological activity from various classes (ITU, DATA, DAPY, α-APA, TIBO, etc.) and the NNIBP.

To further examine the potential for DAPY NNRTIs to have multiple modes for binding to HIV-1 RT, we used molecular dynamics simulations in conjunction with crystallographic refinement as implemented in the simulated annealing/slow-cooling protocol in CNS 1.1.[38] Using different random seeds for calculating initial velocities, the HIV-1 RT/TMC125-R165335 complex was heated to 2500 K and cooled to 0 K in steps of 25 K. Similar simulations were carried out for RT/TMC120-R147681 and RT/R129385 structures.

Acknowledgment. We thank many other members of our current and past research teams (in particular Dequan Sheng, Stefan Sarafianos, Ananda Bhattacharya, Jianping Ding, Andrea Ferris, Daniel Himmel, and Steven Tuske) for advice and encouragement and

the synchrotron support staffs at the Cornell High Energy Synchrotron Source, Brookhaven National Light Source, and the Advanced Photon Source for assistance. E.A. is grateful to the Janssen Research Foundation for financial support and to NIH grants (AI 27690 MERIT Award and P01 GM 56671) for support of RT structural studies. S.H.H. was supported by NIGMS and the NCI.

Note Added after ASAP Posting. This manuscript was released ASAP on 4/6/2004 with an error in the label for the second structure in the bottom row of Scheme 1, errors in the footnote of Table 1, and an error in one of the labels in Figure 6. The correct version was posted on 4/29/2004.

References

(1) De Clercq, E. Highlights in the development of new antiviral agents. *Mini Rev. Med. Chem.* **2002**, *2*, 163−175.
(2) Pauwels, R.; Andries, K.; Desmyter, J.; Schols, D.; Kukla, M. J.; et al. Potent and selective inhibition of HIV-1 replication in vitro by a novel series of TIBO derivatives. *Nature* **1990**, *343*, 470−474.
(3) Pauwels, R.; Andries, K.; Debyser, Z.; Kukla, M. J.; Schols, D.; et al. New tetrahydroimidazo[4,5,1-jk][1,4]-benzodiazepin-2(1H)-one and -thione derivatives are potent inhibitors of human immunodeficiency virus type 1 replication and are synergistic with 2′,3′-dideoxynucleoside analogs. *Antimicrob. Agents Chemother.* **1994**, *38*, 2863−2870.
(4) Pauwels, R.; Andries, K.; Debyser, Z.; Van Daele, P.; Schols, D.; et al. Potent and highly selective human immunodeficiency virus type 1 (HIV-1) inhibition by a series of α-anilinophenylacetamide derivatives targeted at HIV-1 reverse transcriptase. *Proc. Natl. Acad. Sci. U.S.A.* **1993**, *90*, 1711−1715.
(5) Rodgers, D. W.; Gamblin, S. J.; Harris, B. A.; Ray, S.; Culp, J. S.; et al. The structure of unliganded reverse transcriptase from the human immunodeficiency virus type 1. *Proc. Natl. Acad. Sci. U.S.A.* **1995**, *92*, 1222−1226.
(6) Hsiou, Y.; Ding, J.; Das, K.; Clark, A. D., Jr.; Hughes, S. H.; et al. Structure of unliganded HIV-1 reverse transcriptase at 2.7 Å resolution: implications of conformational changes for polymerization and inhibition mechanisms. *Structure* **1996**, *4*, 853−860.
(7) Esnouf, R.; Ren, J.; Ross, C.; Jones, Y.; Stammers, D.; et al. Mechanism of inhibition of HIV-1 reverse transcriptase by non-nucleoside inhibitors. *Nat. Struct. Biol.* **1995**, *2*, 303−308.
(8) Jacobo-Molina, A.; Ding, J.; Nanni, R. G.; Clark, A. D., Jr.; Lu, X.; et al. Crystal structure of human immunodeficiency virus type 1 reverse transcriptase complexed with double-stranded DNA at 3.0 Å resolution shows bent DNA. *Proc. Natl. Acad. Sci. U.S.A.* **1993**, *90*, 6320−6324.
(9) Sarafianos, S. G.; Das, K.; Clark, A. D., Jr.; Ding, J.; Boyer, P. L.; et al. Lamivudine (3TC) resistance in HIV-1 reverse transcriptase involves steric hindrance with β-branched amino acids. *Proc. Natl. Acad. Sci. U.S.A.* **1999**, *96*, 10027−10032.
(10) Huang, H.; Chopra, R.; Verdine, G. L.; Harrison, S. C. Structure of a covalently trapped catalytic complex of HIV-1 reverse transcriptase: implications for drug resistance. *Science* **1998**, *282*, 1669−1675.
(11) Sarafianos, S. G.; Das, K.; Tantillo, C.; Clark, A. D., Jr.; Ding, J.; et al. Crystal structure of HIV-1 reverse transcriptase in complex with a polypurine tract RNA:DNA. *EMBO J.* **2001**, *20*, 1449−1461.
(12) Kohlstaedt, L. A.; Wang, J.; Friedman, J. M.; Rice, P. A.; Steitz, T. A. Crystal structure at 3.5 Å resolution of HIV-1 reverse transcriptase complexed with an inhibitor. *Science* **1992**, *256*, 1783−1790.
(13) Ren, J.; Esnouf, R.; Garman, E.; Somers, D.; Ross, C.; et al. High resolution structures of HIV-1 RT from four RT-inhibitor complexes. *Nat. Struct. Biol.* **1995**, *2*, 293−302.
(14) Esnouf, R. M.; Ren, J.; Hopkins, A. L.; Ross, C. K.; Jones, E. Y.; et al. Unique features in the structure of the complex between HIV-1 reverse transcriptase and the bis(heteroaryl)piperazine (BHAP) U-90152 explain resistance mutations for this non-nucleoside inhibitor. *Proc. Natl. Acad. Sci. U.S.A.* **1997**, *94*, 3984−3989.
(15) Ren, J.; Milton, J.; Weaver, K. L.; Short, S. A.; Stuart, D. I.; et al. Structural basis for the resilience of efavirenz (DMP-266) to drug resistance mutations in HIV-1 reverse transcriptase. *Struct. Fold Des.* **2000**, *8*, 1089−1094.
(16) Lindberg, J.; Sigurdsson, S.; Lowgren, S.; Andersson, H. O.; Sahlberg, C.; et al. Structural basis for the inhibitory efficacy of efavirenz (DMP-266), MSC194 and PNU142721 towards the HIV-1 RT K103N mutant. *Eur. J. Biochem.* **2002**, *269*, 1670−1677.
(17) Hsiou, Y.; Das, K.; Ding, J.; Clark, A. D., Jr.; Kleim, J. P.; et al. Structures of Tyr188Leu mutant and wild-type HIV-1 reverse transcriptase complexed with the non-nucleoside inhibitor HBY 097: inhibitor flexibility is a useful design feature for reducing drug resistance. *J. Mol. Biol.* **1998**, *284*, 313−323.
(18) Hogberg, M.; Sahlberg, C.; Engelhardt, P.; Noreen, R.; Kangasmetsa, J.; et al. Urea-PETT compounds as a new class of HIV-1 reverse transcriptase inhibitors. 3. Synthesis and further structure−activity relationship studies of PETT analogues. *J. Med. Chem.* **1999**, *42*, 4150−4160.
(19) Ren, J.; Diprose, J.; Warren, J.; Esnouf, R. M.; Bird, L. E.; et al. Phenylethylthiazolylthiourea (PETT) non-nucleoside inhibitors of HIV-1 and HIV-2 reverse transcriptases. Structural and biochemical analyses. *J. Biol. Chem.* **2000**, *275*, 5633−5639.
(20) Ding, J.; Das, K.; Tantillo, C.; Zhang, W.; Clark, A. D., Jr.; et al. Structure of HIV-1 reverse transcriptase in a complex with the non-nucleoside inhibitor α-APA R 95845 at 2.8 Å resolution. *Structure* **1995**, *3*, 365−379.
(21) Ding, J.; Das, K.; Moereels, H.; Koymans, L.; Andries, K.; et al. Structure of HIV-1 RT/TIBO R 86183 complex reveals similarity in the binding of diverse nonnucleoside inhibitors. *Nat. Struct. Biol.* **1995**, *2*, 407−415.
(22) Das, K.; Ding, J.; Hsiou, Y.; Clark, A. D., Jr.; Moereels, H.; et al. Crystal structures of 8-Cl and 9-Cl TIBO complexed with wild-type HIV-1 RT and 8-Cl TIBO complexed with the Tyr181Cys HIV-1 RT drug-resistant mutant. *J. Mol. Biol.* **1996**, *264*, 1085−1100.
(23) Tantillo, C.; Ding, J.; Jacobo-Molina, A.; Nanni, R. G.; Boyer, P. L.; et al. Locations of anti-AIDS drug binding sites and resistance mutations in the three-dimensional structure of HIV-1 reverse transcriptase. Implications for mechanisms of drug inhibition and resistance. *J. Mol. Biol.* **1994**, *243*, 369−387.
(24) Hsiou, Y.; Ding, J.; Das, K.; Clark, A. D., Jr.; Boyer, P. L.; et al. The Lys103Asn mutation of HIV-1 RT: a novel mechanism of drug resistance. *J. Mol. Biol.* **2001**, *309*, 437−445.
(25) De Clercq, E. New anti-HIV agents and targets. *Med. Res. Rev.* **2002**, *22*, 531−565.
(26) Cohen, J. Therapies. Raising the limits. *Science* **2002**, *296*, 2322.
(27) Gruzdev, B.; Horban, A.; Boron-Kaczmarska, A.; Gille, D.; Van't Klooster, G.; et al. TMC120, a New Non-Nucleoside Reverse Transcriptase Inhibitor, Is a Potent Antiretroviral in Treatment Naive, HIV-1 Infected Subjects. Presented at the 8th Conference on Retroviruses and Opportunistic Infections, Chicago, 2001.
(28) Gruzdev, B.; Rakhmanova, A.; De Dier, K.; Comhaire, S.; Baede-Van Dijk, P.; et al. TMC125 is a highly potent non nucleoside reverse transcriptase inhibitor (NNRTI) active in antiretroviral therapy (ART)-naive, HIV-1 infected subjects. Presented at the 41st ICAAC, Chicago, 2001.
(29) Gazzard, B.; Pozniak, A.; Arasteh, K.; Staszwski, S.; Rozenbaum, W.; et al. TMC125, A Next-Generation NNRTI, Demonstrates High Potency After 7 Days Therapy in Treatment-Experienced HIV-1-Infected Individuals with Phenotypic NNRTI Resistance. Presented at the 9th Conference on Retroviruses and Opportunistic Infections, Seattle, 2002.
(30) Andries, K.; de Bethune, M.-P.; Ludovici, D.; Kukla, M.; Azijn, H.; et al. R165335-TMC125, a novel non nucleaside reverse transcriptase inhibitor (NNRTI) with nanomolar activity against NNRTI resistant HIV strains. Presented at the 40th ICAAC, Toronto, Canada, 2000.
(31) de Bethune, M.-P.; Andries, K.; Ludovici, D.; Lewi, P.; Azijn, H.; et al. TMC120 (R147681), a next generation NNRTI, has potent in vitro activity against NNRTI-resistant HIV variants. Presented at the 8th Conference on Retroviruses and Opportunistic Infections, Chicago, 2001.
(32) Ludovici, D. W.; De Corte, B. L.; Kukla, M. J.; Ye, H.; Ho, C. Y.; et al. Evolution of anti-HIV drug candidates. Part 3: diarylpyrimidine (DAPY) analogues. *Bioorg. Med. Chem. Lett.* **2001**, *11*, 2235−2239.
(33) Ludovici, D. W.; Kukla, M. J.; Grous, P. G.; Krishnan, S.; Andries, K.; et al. Evolution of anti-HIV drug candidates. Part 1: From α-Anilinophenylacetamide (α-APA) to imidoyl thiourea (ITU). *Bioorg. Med. Chem. Lett.* **2001**, *11*, 2225−2228.
(34) Ludovici, D. W.; Kavash, R. W.; Kukla, M. J.; Ho, C. Y.; Ye, H.; et al. Evolution of anti-hiv drug candidatespart 2: diaryltriazine (DATA) analogues. *Bioorg. Med. Chem. Lett.* **2001**, *11*, 2229−2234.
(35) Lewi, P. J.; de Jonge, M.; Daeyaert, F.; Koymans, L.; Vinkers, M.; et al. On the detection of multiple-binding modes of ligands to proteins, from biological, structural, and modeling. *J. Computer-Aided Mol. Des.* **2003**, *17*, 129−134.
(36) Udier-Blagovic, M.; Tirado-Rives, J.; Jorgensen, W. L. Validation of a Model for the Complex of HIV-1 Reverse Transcriptase with Nonnucleoside Inhibitor TMC125. *J. Am. Chem. Soc.* **2003**, *125*, 6016−6017.
(37) Udier-Blagovic, M.; Watkins, E. K.; Tirado-Rives, J.; Jorgensen, W. L. Activity predictions for efavirenz analogues with the K103N mutant of HIV reverse transcriptase. *Bioorg. Med. Chem. Lett.* **2003**, *13*, 3337−3340.

(38) Brunger, A. T.; Adams, P. D.; Rice, L. M. Recent developments for the efficient crystallographic refinement of macromolecular structures. *Curr. Opin. Struct. Biol.* **1998**, *8*, 606−611.
(39) Balzarini, J.; Karlsson, A.; Perez-Perez, M. J.; Camarasa, M. J.; Tarpley, W. G.; et al. Treatment of human immunodeficiency virus type 1 (HIV-1)-infected cells with combinations of HIV-1-specific inhibitors results in a different resistance pattern than does treatment with single-drug therapy. *J. Virol.* **1993**, *67*, 5353−5359.
(40) Bacheler, L.; Jeffrey, S.; Hanna, G.; D′Aquila, R.; Wallace, L.; et al. Genotypic correlates of phenotypic resistance to efavirenz in virus isolates from patients failing nonnucleoside reverse transcriptase inhibitor therapy. *J. Virol.* **2001**, *75*, 4999−5008.
(41) Ren, J.; Nichols, C.; Bird, L.; Chamberlain, P.; Weaver, K.; et al. Structural mechanisms of drug resistance for mutations at codons 181 and 188 in HIV-1 reverse transcriptase and the improved resilience of second generation non-nucleoside inhibitors. *J. Mol. Biol.* **2001**, *312*, 795−805.
(42) Wang, D. P.; Rizzo, R. C.; Tirado-Rives, J.; Jorgensen, W. L. Antiviral drug design: computational analyses of the effects of the L100I mutation for HIV-RT on the binding of NNRTIs. *Bioorg. Med. Chem. Lett.* **2001**, *11*, 2799−2802.
(43) Ohtaka, H.; Velazquez-Campoy, A.; Xie, D.; Freire, E. Overcoming drug resistance in HIV-1 chemotherapy: the binding thermodynamics of Amprenavir and TMC-126 to wild-type and drug-resistant mutants of the HIV-1 protease. *Protein Sci.* **2002**, *11*, 1908−1916.
(44) Weber, J.; Mesters, J.; Lepsik, M.; Prejdova, J.; Svec, M.; et al. Unusual binding mode of an HIV-1 protease inhibitor explains its potency against multi-drug-resistant virus strains. *J. Mol. Biol.* **2002**, *324*, 739−754.
(45) Hansen, J. L.; Ippolito, J. A.; Ban, N.; Nissen, P.; Moore, P. B.; et al. The structures of four macrolide antibiotics bound to the large ribosomal subunit. *Mol. Cell* **2002**, *10*, 117−128.
(46) Pauwels, R.; Balzarini, J.; Baba, M.; Snoeck, R.; Schols, D.; et al. Rapid and automated tetrazolium-based colorimetric assay for the detection of anti-HIV compounds. *J. Virol. Methods* **1988**, *20*, 309−321.
(47) Clark, A. D. J.; Jacobo-Molina, A.; Clark, P.; Hughes, S. H.; Arnold, E. Crystallization of human immunodeficiency virus type 1 reverse transcriptase with and without nucleic acid substrates, inhibitors and an antibody Fab fragment. *Methods Enzymol.* **1995**, *262*, 171−185.
(48) Otwinowski, Z.; Minor, W. DENZO and SCALEPACK. In *The International Union of Crystallography, Vol. F, Crystallography of Biological Macromolecules*; Rossmann, M. G., Arnold, E., Eds.; Kluwer Academic Publishers: Boston, 2001; pp 226−235.
(49) Jones, T. A.; Zou, J. Y.; Cowan, S. W.; Kjeldgaard Improved methods for binding protein models in electron density maps and the location of errors in these models. *Acta Crystallogr. A* **1991**, *47*, 110−119.
(50) Halgren, T. Merck Molecular Force Field. I. Form, scope, parameterization and performance of MMFF94. *J. Comput. Chem.* **1996**, *17*, 490−519.
(51) Vinkers, H. M.; de Jonge, M. R.; Daeyaert, F. F. D.; Heeres, J.; Koymans, L. M. H.; et al. SYNOPSIS: SYNthesize and OPtimize System in Silico. *J. Med. Chem.* **2003**, *46*, 2765−2773.
(52) Nicholls, A.; Sharp, K. A.; Honig, B. Protein folding and association: insights from the interfacial and thermodynamic properties of hydrocarbons. *Proteins* **1991**, *11*, 281−296.

JM030558S